Science Advances
AAAS

advances.sciencemag.org/cgi/content/full/5/10/eaax1608/DC1

Supplementary Materials for

Epigenetic initiation of the T_H17 differentiation program is promoted by Cxxc finger protein 1

Feng Lin*, Xiaoyu Meng*, Yixin Guo, Wenqiang Cao, Wanlu Liu, Qiming Xia, Zhaoyuan Hui, Jian Chen, Shenghui Hong, Xuliang Zhang, Chuan Wu, Di Wang, Jianli Wang, Linrong Lu, Wenbin Qian, Lai Wei, Lie Wang*

*Corresponding author. Email: wanglie@zju.edu.cn

Published 9 October 2019, *Sci. Adv.* **5**, eaax1608 (2019)
DOI: 10.1126/sciadv.aax1608

This PDF file includes:

Supplementary Materials and Methods

Cell proliferation assay

Naive $CD4^+$ or $CD8^+$ T cells ($CD25^-CD62L^{hi}CD44^{lo}$) from WT and $dLck^{cre}$*Cxxc1*$^{fl/fl}$ mice were sorted, and stained with CellTrace regent (C34557, Invitrogen) according to manufacturer's instructions, then cultured in indicated conditions for 4 days.

Enzyme-Linked Immunosorbent Assay

Interleukin 6 Receptor alpha in the culture supernatant was measured at different time points under Th17 polarization condition, by sandwich enzyme-linked immunosorbent assay (ELISA) (R&D, #DY1830). The concentrations of mouse IL-17A and IFN-γ were measured with ELISA kits (eBioscience) according to the manufacturer's instructions.

RNA isolation and real-time qPCR

Total RNA was extracted using TRIzol reagent (Invitrogen). Real-time qPCR was performed using SYBR Premix Ex TaqTM II on LC480II Real-Time PCR system (Roche, USA) or CFX96 Touch Real-Time PCR (Bio Rad). Results were normalized to β-actin expression.

Deletion of Cxxc1 in $ERT2^{+Cre}$*Cxxc1*$^{fl/f}$ cells

Naive $CD4^+$ T cells ($CD4^+CD25^-CD62L^{hi}CD44^{lo}$) from $ERT2^{+Cre}$*Cxxc1*$^{fl/f}$ mice lymph nodes were sorted and cultured at indicated conditions, at presence of 200 nm 4-hydroxytamoxifen (4-OHT) treatment on the day 0 and day 1.

Western blotting

Cells were lysed in complete lysis-M buffer (Roche; cat.no. 04719956001), and total protein was subjected to SDS–PAGE (6-10%), transferred onto PVDF membranes. Membranes were blocked with 5% non-fat dry milk or 5% BSA (Bio-Rad) in TBS-T and primary antibodies in 5% BSA in TBS-T and HRP coupled secondary antibodies were diluted at 1:5000 in TBS-T. Detection was performed using Fluor Chem E (Cell Biosciences).

Plasmid construction

Recombinant vectors encoding murine IL-6Rα, gp130, STAT3, RORγt and the full-length and truncated/mutated Cxxc1 gene constructs were cloned into pMX-IRES-GFP plasmids. Wild-type STAT3, STAT3 (A662C, N664C), and STAT3 (Y705A) were constructed as described (Pernet et al., 2013). Full-length and truncated/muted Cxxc1 were constructed as described (Cao et al., 2016).

Primers for Plasmid construction:

Gene	Forward Primer	Reverse Primer
IL6Ra	GAATTCCACCGATCTGAGCCACG	GCGGCCGCGGACCCGCATGAGAAACT
gp130	GCGGCCGCCTGCAAGATGTCAGCACCAA	TACGTATCAGGAGCCAGTCCTTCACT
Cxxc1(1-656)	GAATTCATGGAAGGAGATGGCTCAGA	GCGGCCGCTAGTCAGCGGTCGGCACTAGA
Cxxc1 (1-367)	GAATTCATGGAAGGAGATGGCTCAGA	GCGGCCGCTTACCTCTCTGGGTGTTTCCATT
Cxxc1 (361-656)	GAATTCAATGTGGAAACACCCAGAGAGGG	A GCGGCCGCTAGTCAGCGGTCGGCACTAGA
Cxxc1 (C169A)	ACGATCAGCTCGGATGGCTGGTGAGTGCGAGGC	GCCTCGCACTCACCAGCCATCCGAGCTGATCGT
Cxxc1 (C375A)	TGCATCTCTCCCGCAGGCCCTGGGGCCTGGCTGTGT	ACACAGCCAGGCCCCAGGGCCTGCGGGAGAGATGCA
RORγt	GAATTCAAACACTGGGGGAGAGCTTT	CGGCCGCGGTCAGAGGGCTGAAGGAAA

Primers for qPCR:

Primers for ChIP-qPCR:

Gene	Location	Forward Primer	Reverse Primer
IL-6Rα	TSS	ACCTCCACCGCGTCAGCACA	TGGTTCCGTTCGCAGAGTGAG
gp130	TSS	GCCAGAGCTTCGAGCCATCC	GGCCCTGTTCTTCTCACCTTCC
BATF	TSS	AGACAGAACCGAGGTCAGGG	ACTGCTGGAGTTACCGAGGC
IRF4	TSS	GGCTTCCTCCCGCCTCCAAA	CTGCCCGTCTCCAAGTTCAT
Runx1	TSS	CCGCCTATGCTGTGGGTTGA	GCCTGGCAGTGTCAGAAGTG
Satb1	TSS	GCCCAGTCCTCCCGAATGTC	GTCCCGCTTCTTTGCTCCCT
Rorc	+10kb	TGCTGCTAAGAGGATGAAGA	CCTGGGCTGAGGAAACGATA
Rora	+400kb	TTGAGATGATTGCTGCTGAT	TGTCCTGTGGCTGAGGTTTT
IL21	TSS	ATTCCAGTTTTCAGCATTCA	GTCAGACAAACCAGGTGAGG

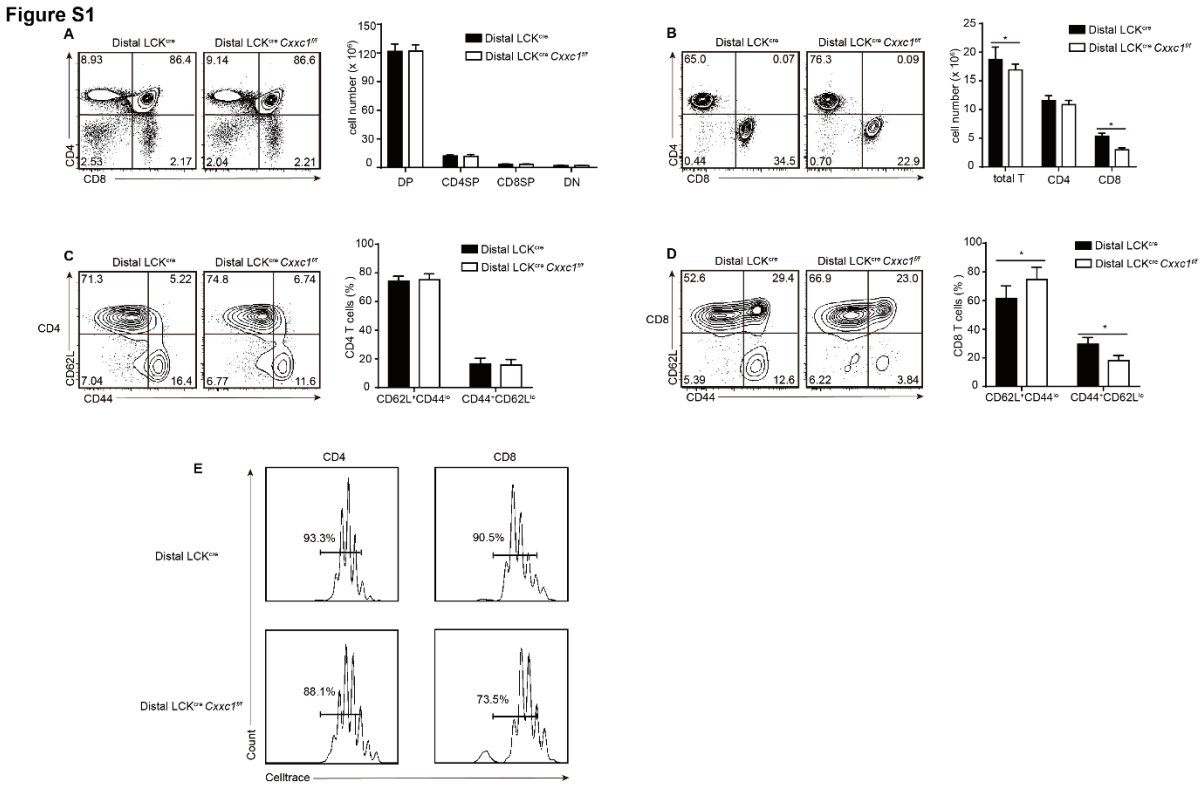

Fig. S1. Phenotype of Cxxc1 conditional KO mice.

Flow cytometry assay of $CD4^+$ and $CD8^+$ from Thymus. And absolute cell numbers of DN, DP, $CD4^+$ and $CD8^+$ SP thymocyte subpopulations.

(A) Splenocytes from dLck^{cre}*Cxxc1*$^{fl/fl}$ and WT mice were stained for CD4 and CD8 analyzed by flow cytometry. And absolute cell numbers of Total T, $CD4^+$ and $CD8^+$ T-cell subsets.

(**C**, **D**) Splenocytes from dLck^{cre}*Cxxc1*$^{fl/fl}$ and WT mice were stained for CD4, CD8, CD44, and CD62L and analyzed by flow cytometry.

(**E**) CellTrace staining of naive $CD4^+$ or $CD8^+$ T cells from dLck^{cre}*Cxxc1*$^{fl/fl}$ and WT mice after 4 days of stimulation in the presence of anti-CD3 and anti-CD28 antibody. The statistical significance was calculated by Student's *t*-test. *, $P \leq 0.05$. Error bars show the mean ± SD. Data are from six-mice analysis.

Figure S2

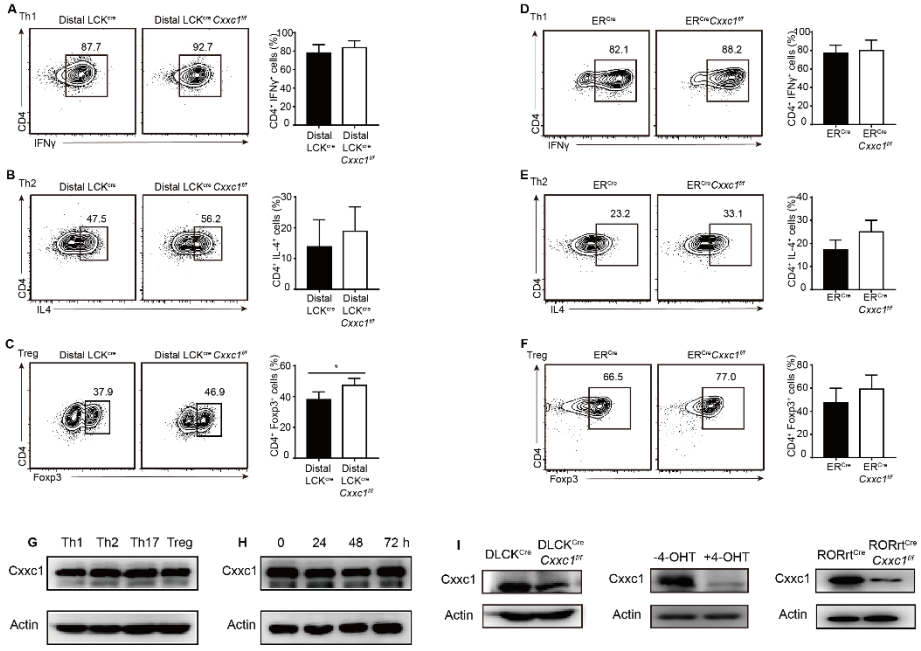

Fig. S2. (related to Fig. 1). Analysis of T cell differentiation in vitro from WT and Cxxc1-deficient mice. (**A-C**) Naive CD4^{+}T cells were sorted from dLck^{cre}*Cxxc1*$^{fl/fl}$ and WT mice and then polarized into (A) Th1 cells, (B) Th2 cells, (C) iTreg cells for 4 days in vitro, and analyzed by intracellular staining after restimulation. These experiments were repeated for at least six times with the consistent results.
(**D-F**) Naive CD4^{+} T cells from ERT2^{cre}*Cxxc1*$^{fl/fl}$ and WT mice were polarized into (D) Th1 cells, (E) Th2 cells, (F) iTreg cells, at presence or absence of 4-OHT for 4 days in vitro, and then analyzed by intracellular cytokines staining after restimulation. These experiments were repeated for at least five times.
(**G, H**) The expression levels of Cxxc1 protein in T helper subsets and different stages of Th17 cells.
(**I**) Detection of Cxxc1 protein deletion in Th17 cells (72 hr). DLck^{cre} (left), ERT2^{+Cre} (middle), RORγt^{cre} (right). One of four experiments is shown.
The statistical significance was calculated by Student's *t*-test. Error bars show the mean ± SD.

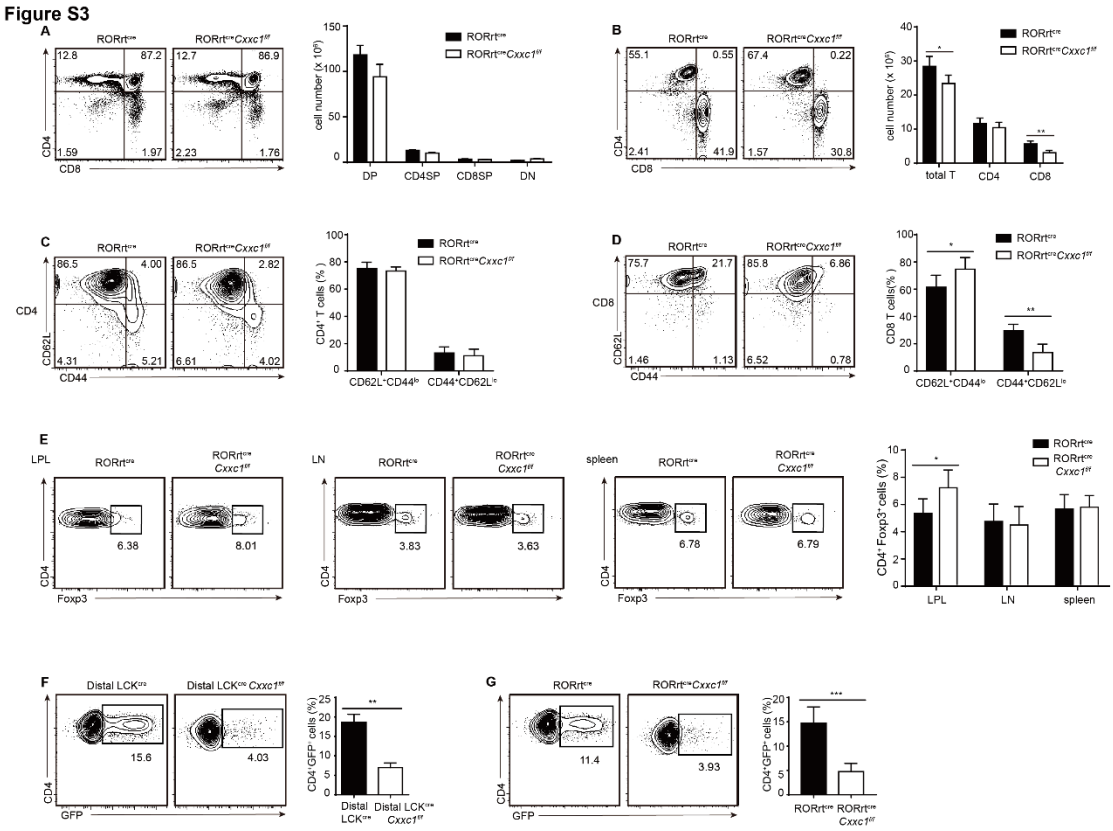

Fig. S3. Phenotype of RORγt^{cre}*Cxxc1*$^{wt/wt}$ and RORγt^{cre}*Cxxc1*$^{fl/fl}$ mice.

(**A**) Flow cytometry assay of CD4$^+$ and CD8$^+$ from Thymus. And absolute cell numbers of DN, DP, CD4$^+$ and CD8$^+$ SP thymocyte subpopulations. One of five experiments is shown.

(**B**) Splenocytes from RORγt^{cre}*Cxxc1*$^{fl/fl}$ and WT mice were stained for CD4 and CD8 and analyzed by flow cytometry. And absolute cell numbers of Total T, CD4$^+$ and CD8$^+$ T-cell subsets. One of five experiments is shown.

(**C, D**) Splenocytes from RORγt^{cre}*Cxxc1*$^{fl/fl}$ and WT mice were stained for CD4, CD8, CD44, and CD62L and analyzed by flow cytometry. One of five experiments is shown.

(**E**) Frequencies of Foxp3 in RORγt^{cre}*Cxxc1*$^{fl/fl}$ and WT mice, in LPL, lymph nodes and spleen. One of five experiments is shown.

(**F, G**) Naive CD4$^+$T cells from IL17A^{eGFP} reporter of dLck^{cre}*Cxxc1*$^{fl/fl}$, RORγt^{cre}*Cxxc1*$^{fl/fl}$ or WT mice were differentiated into Th17 cells with IL-6 and TGF-β1, and then CD4$^+$ GFP$^+$ cells were analyzed by flow cytometry after 96 hours. One of four experiments is shown.

The statistical significance was calculated by Student's *t*-test. *, $P \leq 0.05$; **, $P \leq 0.01$; ***, $P \leq 0.001$. Error bars show the mean ± SD.

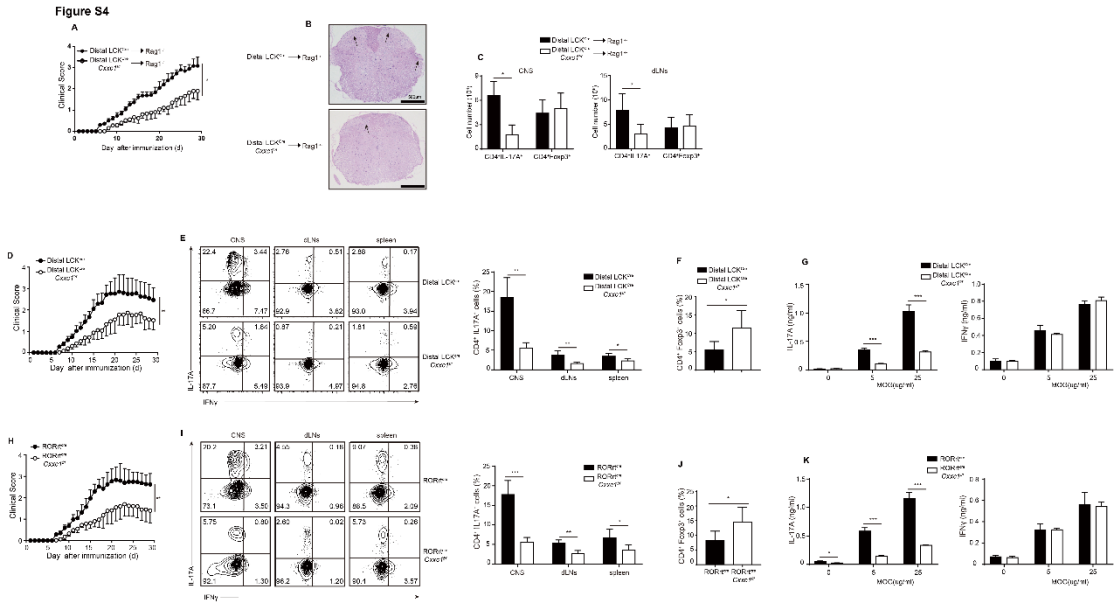

Fig. S4. (related to Fig. 2). Cxxc1 deficiency restricts T cell–mediated autoimmunity.

(A) Mean clinical scores for EAE in Rag1$^{-/-}$ recipients of dLck^{cre}*Cxxc1*$^{fl/fl}$ (n=12) and WT (n=10) naive CD4^{+} T cells after being immunized with $MOG_{35–55}$, CFA and pertussis toxin. Data are summed from three independent experiments.

(B) Representative histology of the spinal cord of Rag1$^{-/-}$ mice after EAE induction (day 22). hematoxylin and eosin [H&E].

(C) On day 20 after EAE induction of Rag1$^{-/-}$ hosts, CD4^{+} T cells were analyzed from the leukocytes isolated from the CNS, draining lymph nodes, and further analysed for the expression of IL-17A^{+} and Foxp3^{+} cells in Rag1$^{-/-}$ hosts. One of five experiments is shown.

(**D-G**) EAE model in dLck^{cre}*Cxxc1*$^{fl/fl}$ (n=11) or WT (n=9) mice. Mean clinical scores (**D**), frequency of IL-17A^{+} and IFNγ^{+} T cells in leukocytes isolated from the CNS, draining lymph nodes and spleen (**E**), frequency of Foxp3^{+} cells from CNS-infiltrating lymphocytes (**F**), Splenocytes were stimulated for 3 d with MOG peptide (0, 5, 25 μg/mL), and cytokine production was measured by ELISA (**G**).

(**H-K**) EAE model in RORγt^{cre}*Cxxc1*$^{fl/fl}$ (n=13) or WT (n=10) mice. Mean clinical scores (**H**), frequency of IL-17A^{+} and IFNγ^{+} T cells in leukocytes isolated from the CNS, draining lymph nodes and spleen (**I**), frequency of Foxp3^{+} cells from CNS-infiltrating lymphocytes (**J**), Splenocytes were stimulated for 3 d with MOG peptide (0, 5, 25 μg/mL), and cytokine production was measured by ELISA (**K**).

The statistical significance was calculated by Student's *t*-test. *, $P \leq 0.05$; **, $P \leq 0.01$; ***, $P \leq 0.001$. Error bars show the mean ± SD.

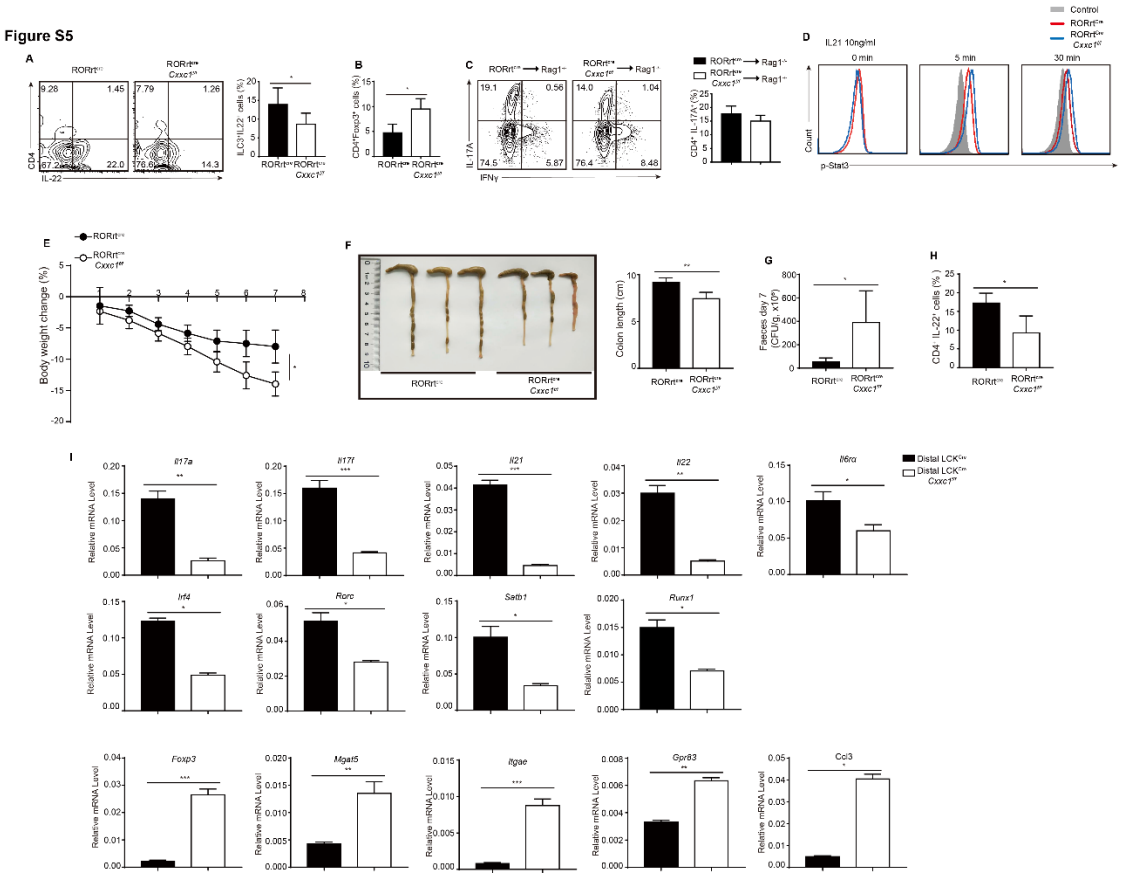

Fig. S5. Cxxc1 deficiency increased sensitivity to *C. rodentium* infection.

(**A**) FACS analysis of IL-22 expression by ILC3 ($Lin^{-}ROR\gamma t^{+}$) from isolated LPLs in $Rag1^{-/-}$ recipients of naive $CD4^{+}$ T cells from $ROR\gamma t^{cre}Cxxc1^{fl/fl}$ (n=12) or WT (n=11) mice after oral inoculation with *C. rodentium* at day 7. One of four experiments is shown.

(**B, C**) FACS analysis of Foxp3 and IL-17A expression from isolated LPLs in $Rag1^{-/-}$ recipients after oral inoculation with *C. rodentium* at day 7. One of four experiments is shown.

(**D**) The level of STAT3 phosphorylation by IL-21 stimulation of $ROR\gamma t^{cre}Cxxc1^{fl/fl}$ or WT cells. One of four experiments is shown.

(**E-H**) *C. rodentium* infection in $dLck^{cre}Cxxc1^{fl/fl}$ (n=9) or WT (n=8) mice. Body weight changes of mice after oral inoculation with *C. rodentium* at the indicated time points (**E**), Colon length at day 7 (**F**), *C. rodentium* CFUs in the colon 7 d after inoculation (**G**), FACS analysis of IL-22 expression at day 7 after inoculation. One of five experiments is shown.

(**I**) Naive $CD4^{+}$ T cells ($CD4^{+}CD25^{-}CD62L^{hi}CD44^{lo}$) from WT and $dLck^{cre}Cxxc1^{fl/fl}$ mice were differentiated in the presence of TGF-β1 and IL-6 (Th17) for 72 hr, and the expression of the selected transcripts was quantified by quantitative real-time PCR. One of five experiments is shown.

Error bars show the mean ± SD. *, $P \leq 0.05$; **, $P \leq 0.01$; ***, $P \leq 0.001$ in a Student's *t*-test. (Photo Credit: Feng Lin, Institute of Immunology, Zhejiang University School of Medicine).

Figure S6

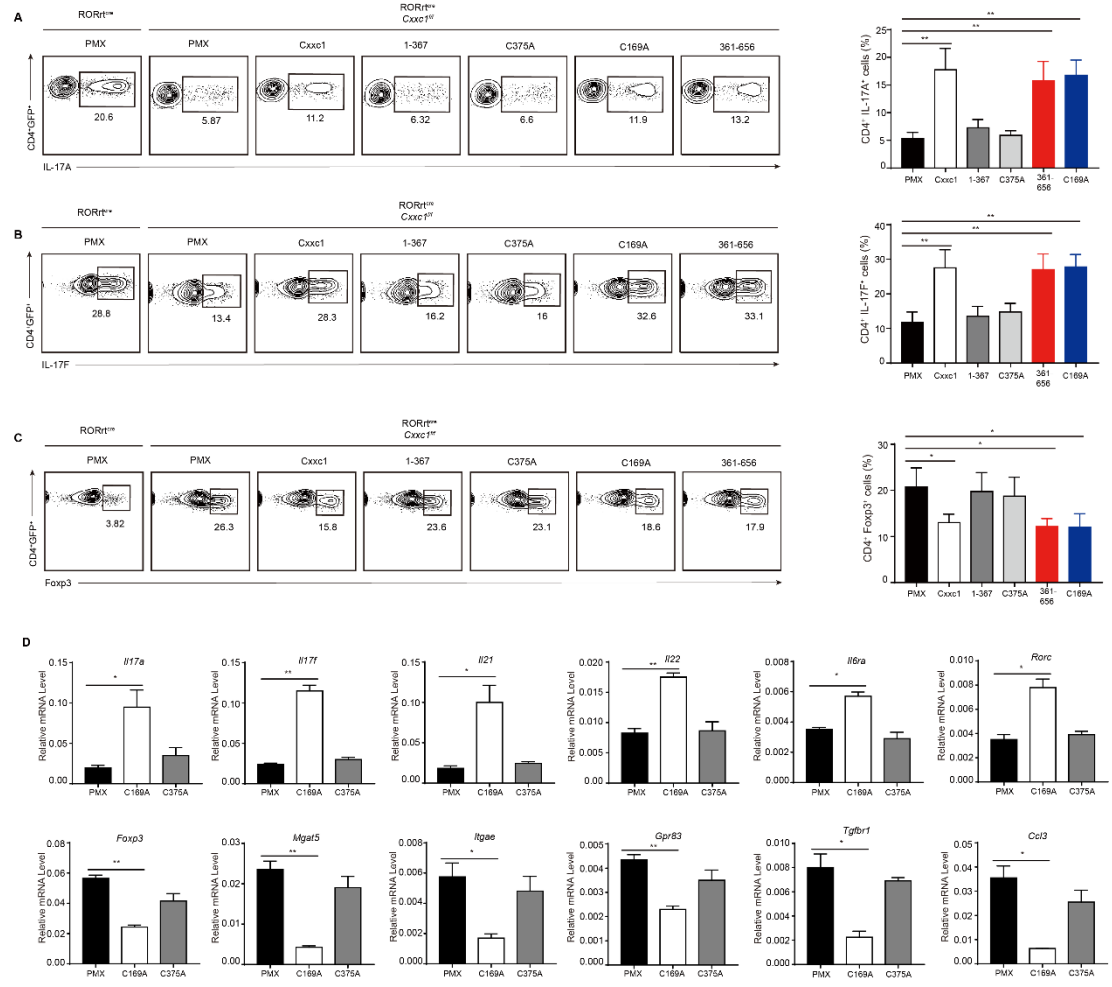

Fig. S6. Cxxc1 regulates T_H17 differentiation with its H3K4me3 function.

(**A-C**) Sorted naive $CD4^+$ T cells were differentiated into Th17 cells in the presence of TGF-β1 and IL-6, 20-24 hr later the cells were transfected with indicated retrovirus, then IL-17A (A) and IL-17F (B), foxp3 (C) were measured by gated $CD4^+GFP^+$ cells after infected retrovirus for 72 hr. One of five experiments is shown.

(**D**) CKO Th17 cells were transfected with indicated retrovirus for 72 hr, then gene expression changes were measured by real-time PCR. One of four experiments is shown.

The statistical significance was calculated by Student's *t*-test. *, $P \leq 0.05$; **, $P \leq 0.01$. Error bars show the mean ± SD.

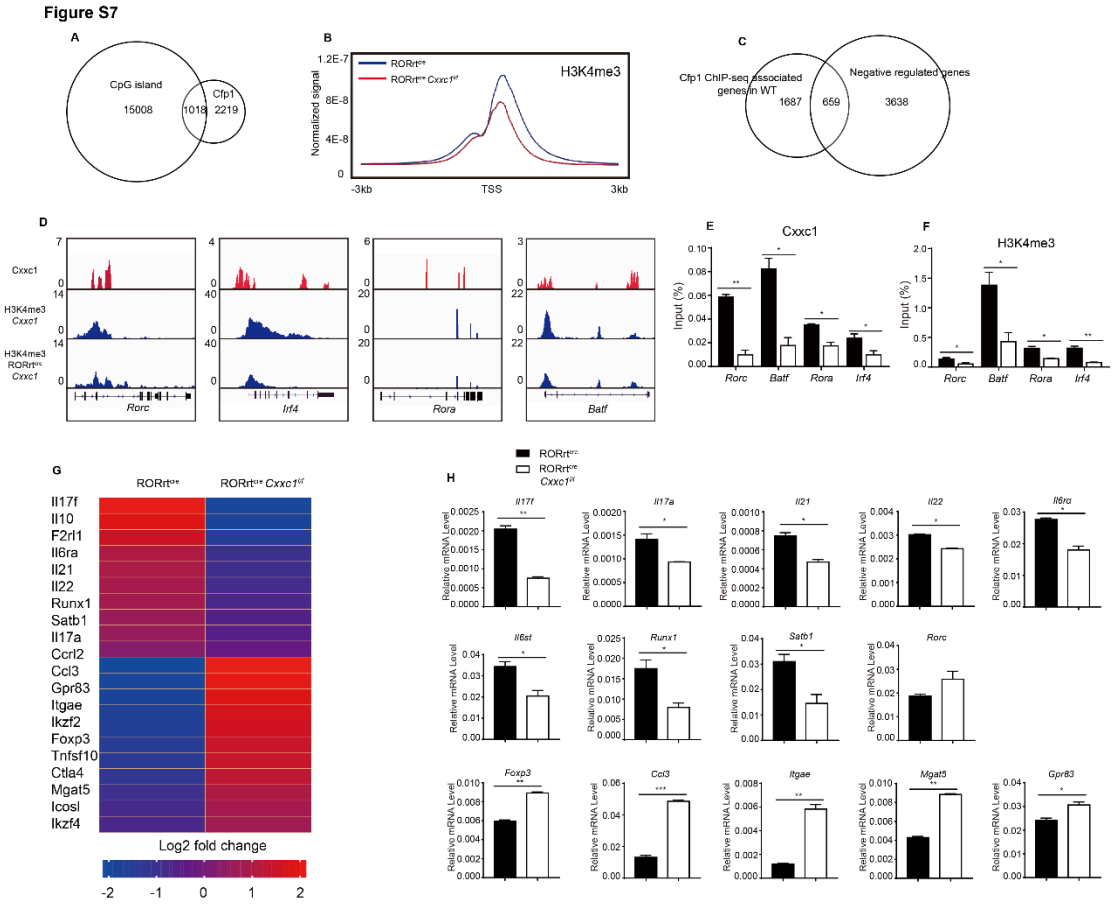

Fig. S7. Genome-wide maps of Cxxc1 binding and H3K4me3 modifications in T_H17 cells differentiated from naive CD4$^+$ T cells with TGF-β1 and IL-6 for 24 hours.

(**A**) The number of genomic regions at which CGIs and Cxxc1-binding sites were colocalized.

(**B**) Distribution of H3K4me3 modifications around 3 kb regions flanking the TSS of all RefSeq (mm10) genes in WT and *Cxxc1*-deficient Th17 cells.

(**C**) Overlapped regions between Cxxc1-binding sites, and RNA-seq up regulated genes in WT and *Cxxc1*-deficient Th17 cells.

(**D**) IGV browser view of Cxxc1-binding peaks (red) in WT Th17 cells and H3K4me3 markers (blue) in WT and *Cxxc1*-deficient Th17 cells.

(**E, F**) Naive WT CD4$^+$ T cells were sorted and cultured under Th17 differentiation conditions (TGF-β plus IL-6) for 24 hr, and ChIP-qPCR analysis of Cxxc1 binding or H3K4me3 modifications at the indicated gene loci were performed.

(**G**) Naive CD4$^+$ T cells (CD4$^+$CD25$^-$CD62L^{hi}CD44^{lo}) from WT and RORγt^{cre}*Cxxc1*$^{fl/fl}$ mice were differentiated in the presence of TGF-β1 and IL-6 (Th17) for 24 hr. Total RNA from the cells was analyzed by RNA-seq (STAR method). Heatmap of fold change (log2) for differentially expressed genes (FDR < 0.05 in Th17 is shown).

(**H**) The expression of the selected transcripts was quantified in Th17 cell samples differentiated from naive CD4$^+$ T cells with TGF-β1 and IL-6 for 24 hr by quantitative

real-time PCR.
Error bars show the mean ± SD. *, $P \leq 0.05$; **, $P \leq 0.01$; ***, $P \leq 0.001$ in a Student's *t*-test.

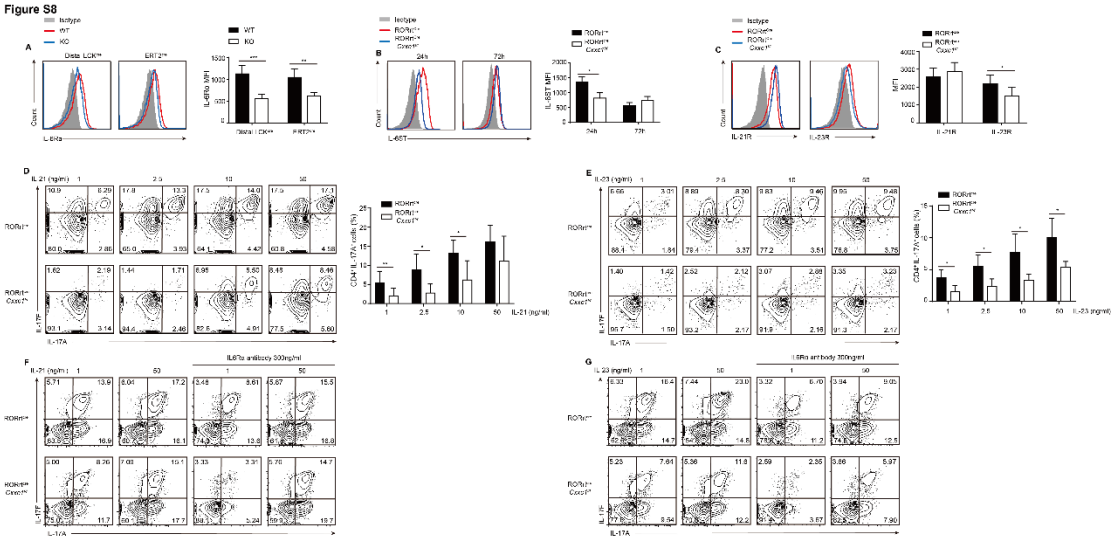

Fig. S8. (related to Fig. 5). The IL-6–Stat3 signaling pathway was defective after Cxxc1 deletion.

(**A**) Naive CD4$^+$ T cells (CD4$^+$CD25$^-$CD62L^{hi}CD44^{lo}) from dLck^{cre}*Cxxc1*$^{fl/fl}$ and WT mice or ERT2^{+cre}*Cxxc1*$^{fl/fl}$ mice were differentiated into Th17 cells with IL-6 and TGF-β1, then the expression of IL-6Rα was measured by flow cytometry(left), and mean fluorescence intensity (MFI) of IL-6Rα was measured (right). 4-OHT were added to delete Cxxc1 in ERT2^{+cre}*Cxxc1*$^{fl/fl}$ cells. One of four experiments is shown.

(**B**) Naive CD4$^+$T cells from RORγt^{cre}*Cxxc1*$^{fl/fl}$ and WT mice were differentiated into Th17 cells with IL-6 and TGF-β1, then the expression of IL-6ST was measured by flow cytometry (left), and mean fluorescence intensity (MFI) of IL-6ST at different time points was measured (right). One of four experiments is shown.

(**C**) Naive CD4$^+$T cells from RORγt^{cre}*Cxxc1*$^{fl/fl}$ and WT mice were differentiated into Th17 cells with IL-6 and TGF-β1, then the expression levels of IL-21R and IL-23R were measured by flow cytometry (left), and mean fluorescence intensity (MFI) of IL-21R and IL-23R was measured (right). One of four experiments is shown.

(**D**, **E**) WT and RORγt^{cre}*Cxxc1*$^{fl/fl}$ naive CD4$^+$T cells were cultured in the presence of TGF-β1 and varying concentrations of IL-21 (D) or IL-23 (E) for 72 hours, and then the expression levels of IL-17A and IL-17F were analyzed. One of five experiments is shown.

(**F**, **G**) WT and RORγt^{cre}*Cxxc1*$^{fl/fl}$ naive CD4$^+$T cells were cultured in the presence of TGF-β1 and indicated concentrations of IL-21 (F) or IL-23 (G) without or with 300ng/ml of IL-6Rα antibody for 72 hours, and then the expression levels of IL-17A and IL-17F were analyzed. One of four experiments is shown.

The statistical significance was calculated by Student's *t*-test. *, $P \le 0.05$; **, $P \le 0.01$; ***, $P \le 0.001$. Error bars show the mean ± SD.

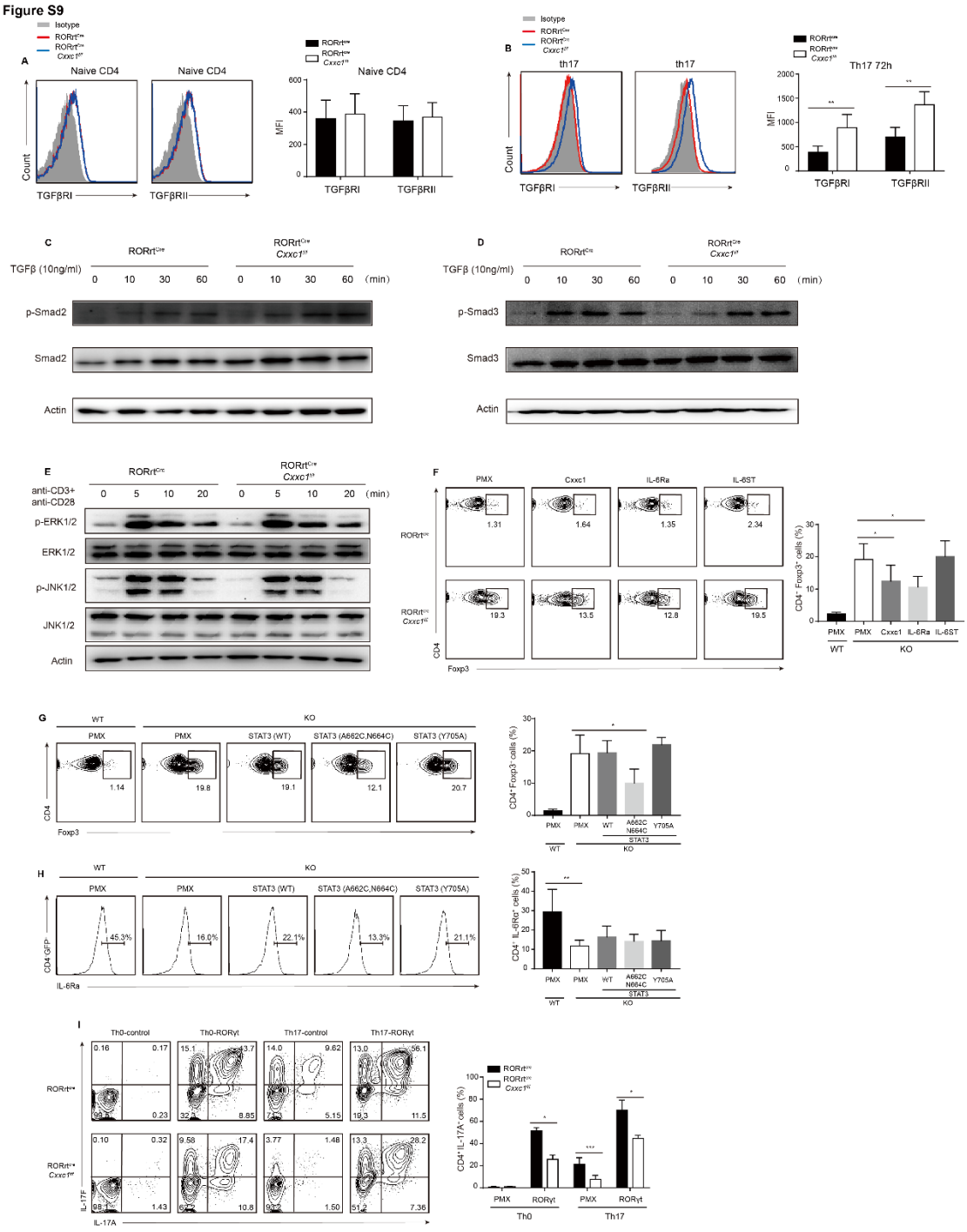

Fig. S9. (related to Fig. 6). Cxxc1 mediates T_H17 cell differentiation by mediating IL-6Rα expression. (**A**) Naive CD4$^+$T cells from RORγt^{cre}*Cxxc1*$^{fl/fl}$ and WT mice were sorted, then the expression levels of TGFβ receptor I and II were measured by flow cytometry(left), and mean fluorescence intensity (MFI) of TGFβ receptor I and II were measured (right). One of four experiments is shown.

(**B**) Naive CD4$^+$T cells from RORγt^{cre}*Cxxc1*$^{fl/fl}$ and WT mice were differentiated into Th17 cells with IL-6 and TGF-β1 for 72 hours, then the expression levels of TGFβ

receptor I and II were determined by flow cytometry, and the mean fluorescence intensity (MFI) of TGFβ receptor I and II were measured (right). One of five experiments is shown.

(**C**, **D**) RORγt^{cre}*Cxxc1*$^{fl/fl}$ and WT naive CD4^{+}T cells were stimulated with 10 ng/ml TGF-β1 as indicated time, then phosphorylated and total smad2 and smad3 proteins were detected by western blot assays. One of four experiments is shown.

(**E**) Naive CD4^{+} T cells sorted from wild-type or RORγt^{cre}*Cxxc1*$^{fl/fl}$ mice were stimulated with anti-CD3 (3μg/ml) plus anti-CD28 (3μg/ml) antibodies for indicated time. The cell lysates were subjected to Western Blot using indicated antibodies. One of four experiments is shown.

(**F**) Naive CD4^{+} T cells from WT and RORγt^{cre}*Cxxc1*$^{fl/fl}$ mice were differentiated into Th17 cells in the presence of TGF-β1 and IL-6, 20-24 hr later the cells were transfected with indicated retrovirus (Mock, Cxxc1, IL6Ra and IL-6ST), then Foxp3 were measured by gated CD4^{+} GFP^{+} cells after infected retrovirus for 72 hr. One of five experiments is shown.

(**G**, **H**) Sorted naive CD4^{+} T cells from WT and RORγt^{cre}*Cxxc1*$^{fl/fl}$ mice were differentiated into Th17 cells in the presence of TGF-β1 and IL-6, 20-24 hr later the cells were transfected with indicated retrovirus (Mock, STAT3 (WT), STAT3 (A662C, N664C) and STAT3 (Y705A)), then Foxp3 (G) and IL-6Rα (H) were measured by gated CD4^{+} GFP^{+} cells after infected retrovirus for 72 hr. One of four experiments is shown.

(**I**) Sorted naive CD4^{+} T cells from WT and RORγt^{cre}*Cxxc1*$^{fl/fl}$ mice were polarized into Th17 cells in the presence of TGF-β1 and IL-6, 20-24 hr later the cells were transfected with indicated retrovirus (Mock, RORγt). IL-17A and IL-17F levels were then measured by gated CD4^{+}GFP^{+} cells after retrovirus infection for 72 hr. One of five experiments is shown.

The statistical significance was calculated by Student's *t*-test. *, $P \leq 0.05$; **, $P \leq 0.01$; ***, $P \leq 0.001$. Error bars show the mean ± SD.

Table S1

Down regulated genes in Cfp1 deficient Th17 cells

Ccna2	Hmgb2	1700016K19Rik	Ly6e
Gm572	Ms4a6b	Gimap4	Arl4c
Clspn	H2-T3	Mcf2l	Rdx
Il2	Emp1	Tymp	Tmem30b
Grk4	Cxxc1	Rcc1	Acsf3
Dapl1	Rapgef4	Pfdn5	Cenpu
4930512M02Rik	Shox2	Eya2	Klhdc1
Lrr1	Prdm8	Tshz1	Cdh15
Inhba	Fbxo5	Pced1b	Cd28
Kif11	Olfr1423	Maml3	Acoxl
Fasl	Rmi2	Tdrp	Kdsr
Ncs1	Trdmt1	Lrrc32	Prmt6
Meis1	Wee1	Ust	Scrib
Fcgr1	Mdp1	Timm22	Hmgb1
Dtl	Parp16	Hs2st1	Map4k5
Bub1	Bard1	Slc16a10	Sclt1
Il7r	Kif2c	Klf2	Dennd2d
Esco2	Tsen2	Srm	Stk38
Nrep	Klf4	Dgka	Ccsap
Il10	Adap1	Helq	Kbtbd11
Il21	Eif2b3	Rtkn2	Tle3
Emilin1	Mfsd2a	Clpb	Dbp
Zfp13	Hist1h4a	Cep152	Gimap8
Mxra7	Mtss1	Satb1	Ier2
Kif15	1700001O22Rik	Eef2kmt	Gclm
Ccdc80	Trappc9	Rac2	Ttc7b
Cenpf	Grk6	Fam105a	Fos
Fam161a	Wnt5b	Me2	Slc20a1
Fndc1	Gpr183	Snapin	Ezh2
Zfp521	Ubash3a	Skap1	Rpap3
Dmrta1	Rundc3b	Stx18	Hnrnpdl
Thy1	Lmna	Scml4	Runx1
Fosb	Pik3ip1	Zmynd19	Dnajc6
Top2a	Lhx9	Cdk8	Dgkz
Dut	Sox6	Cd44	Tasp1
Pcx	Sfxn1	Crebl2	Nup210
Ybey	Ncln	Tmem242	Ceacam2
Dnmt3b	Il6ra	Limd2	Sh2d3c
Sell	Noct	Habp4	Bend4
Spry1	Hist1h2br	Sgk3	
S1pr1	St8sia6	Gm5458	
Zdhhc14	Cmah	Timm13	